Response of a Preexisting Cyclonic Ocean Eddy to a Typhoon

ZHUMIN LU

State Key Laboratory of Tropical Oceanography, South China Sea Institute of Oceanology, Chinese Academy of Sciences, Guangzhou, and State Key Laboratory of Satellite Ocean Environment Dynamics, Second Institute of Oceanography, State Oceanic Administration, Hangzhou, China

GUIHUA WANG

Institute of Atmospheric Sciences, Department of Environmental Science and Engineering, Fudan University, Shanghai, and State Key Laboratory of Satellite Ocean Environment Dynamics, Second Institute of Oceanography, Hangzhou, China

XIAODONG SHANG

State Key Laboratory of Tropical Oceanography, South China Sea Institute of Oceanology, Chinese Academy of Sciences, Guangzhou, China

(Manuscript received 12 February 2016, in final form 1 June 2016)

ABSTRACT

The three-dimensional responses of a cyclonic ocean eddy (COE) for 1–2 months following a typhoon were investigated using altimeter data and numerical experiments. Two significant features were found: 1) the cyclonic eddy was enhanced, and the three-dimensional structure was changed, and 2) the cyclonic eddy underwent two processes: elliptical deformation and reaxisymmetrization in the horizontal plane. These two features are generally associated with typhoon-induced upwelling and the dynamic processes of eddy adjustment. These results imply that the local ocean processes can be affected by a typhoon through low-frequency response.

1. Introduction

The oceanic response to a typhoon or hurricane is an important topic in the oceanographic community. Because of the ubiquitous mesoscale processes in the upper ocean, the interaction between typhoons and mesoscale oceanic features such as cyclonic ocean eddies (COEs) has attracted considerable attention (e.g., Jaimes et al. 2011; Sun et al. 2014; Walker et al. 2005; Zheng et al. 2008, 2010). COEs can enhance typhoon-induced surface cooling (e.g., Walker et al. 2005; Zheng et al. 2008) through the combined effects of upwelling, wind mixing, and the enhancement of shear-driven mixing at the base of mixed layer (Jaimes et al. 2011). Furthermore, the increased surface cooling due to the preexistence of a COE can weaken the intensity of a typhoon through a negative feedback mechanism (Chang and Anthes 1978; Black and Holland 1995; Schade and Emanuel 1999).

Although the lifetime of an eddy is usually longer than that of a typhoon, COEs themselves can be altered by typhoons. Sun et al. (2014) illustrated the effects of supertyphoons on the strength, spatial area, and kinetic energy of COEs. Shang et al. (2015) compared the eddy kinetic energy and available gravitational potential energy of COEs before and after typhoons and found that the energy of a COE can be increased by a slow-moving typhoon. Some observations have found the long-lived biophysical response in COEs by remote sensing and using Argo floats (Sun et al. 2010, 2012; Walker et al. 2014); however, the dynamic processes need to be investigated further by numerical model. Eddy structure is important for ocean chlorophyll (Chelton et al. 2011), biogeochemistry (Benitez-Nelson et al. 2007), and some physical process such as eddy stirring (Legal et al. 2007), but few studies emphasize the evolution of eddy structure after a typhoon. The principal aim of this study was

Corresponding author address: Dr. Zhumin Lu, State Key Laboratory of Tropical Oceanography, South China Sea Institute of Oceanology, Chinese Academy of Sciences, West Xingang Road No. 164, Guangzhou 510301, China.
E-mail: luzhumin@scsio.ac.cn

DOI: 10.1175/JPO-D-16-0040.1

to resolve the three-dimensional evolution of a COE after perturbation by a typhoon using altimeter data and numerical experiments.

2. Data, models, and methods

The daily altimetry-based sea surface height anomaly (SSHA) products, that is, TOPEX/ERS merged data from Archiving, Validation, and Interpretation of Satellite Oceanographic data (AVISO), were used to analyze the development of the COE. Potential vorticity anomaly (PVA) was used to analyze the evolution of the COE spatial structure. Potential vorticity (PV) is defined as

$$q = -\frac{\zeta + f}{\rho}\frac{\partial \rho}{\partial z}, \tag{1}$$

where ζ is the relative vorticity, f is planetary vorticity, and ρ is seawater density. PVA is represented as

$$\mathrm{PVA} = q - q_0, \tag{2}$$

where q_0 is the initial PV of the COE before the typhoon arrived. Both PVA and PV are equally conservative, but the zero PVA contour is a more convenient tool for identifying the eddy core than PV contour.

Using the Hybrid Coordinate Ocean Model (HYCOM; Bleck 2002), a flat-bottom ocean on the f or β plane was customized to investigate the effect of a typhoon on the COE. The depth of the model ocean was set to be 4000 m, with a vertical resolution of 30 layers. The thickness of the first layer was set at 10 m, and the thickness of the other layers increased geometrically with depth. The initial stratification was obtained from the *World Ocean Atlas 2009* (*WOA09*) seasonal-mean temperature–salinity (T–S) data. The initial T–S field was horizontally uniform in the model domain. To idealize our experiment, we used the mesoscale eddy model derived from Zhang et al. (2013). We placed the origin at the center of the COE with x, y, and z pointing eastward, westward, and upward, respectively. The day when the COE encountered the typhoon was set as $t = 0$. To prevent the reflected waves from interacting with the COE, the horizontal model domain (−3000, 2500 km) × (−2200, 2200 km) was divided into an inner zone covering (−1000, 2500 km) × (−700, 700 km) with a 10 km × 10 km resolution and an outer zone with variable grids. The model ocean was forced only by a wind stress field from the daily QuikSCAT wind data for Typhoon Lupit taken on 28 November 2003. The track and the moving speed of Typhoon Lupit are from the "best-track" data supplied by Japan Meteorological Agency (JMA). The 30-day spinup of the mesoscale eddy model was executed with no initial forcing in the ocean model. The model typhoon was initially placed away from the COE and moved from east to west.

3. Results

a. *Evolution of a COE after perturbation by a typhoon*

A COE located at 16.5°N, 132°E encountered Typhoon Lupit on 28 November 2003 in the western Pacific Ocean. Altimetry observation showed the evolution of a COE in response to Typhoon Lupit (Fig. 1a), and two robust features were found. First, the COE was enhanced and enlarged by Typhoon Lupit; 30 days after Lupit passed by the COE, the eddy amplitude and radius increased to a maximum of 11 cm and 50 km (Fig. 1a4), respectively. Second, the eddy deformed from a circle to an ellipse with a major axis that aligned with the track (Fig. 1a3) and then readjusted to be circular once again (Fig. 1a4). The first and second processes are defined as elliptical deformation and reaxisymmetrization, which are caused by horizontal current shear or strain and dynamic adjustments in decaying geostrophic turbulence, respectively (Carton 2001). The initial diameter of the circular eddy was approximately 220 km at $t = -7$ days (Fig. 1a1), and the major and minor axes of the elliptical eddy were approximately 355 and 138 km, respectively, at $t = 10$ days (Fig. 1a3). Once the reaxisymmetrization finished, the COE reached a new quasi-steady state with a diameter of 308 km at $t = 28$ days.

The model simulation repeated the two features observed from the altimeter data (Fig. 1b). The cyclonic eddy was strengthened with a maximum increase in the eddy amplitude and radius of approximately 13 cm and 50 km, respectively. The eddy also underwent elliptical deformation and reaxisymmetrization processes. The initial diameter of the circular eddy was approximately 220 km at $t = -7$ days, and the length of major and minor axes of the elliptical eddy were approximately 279 and 151 km, respectively, at $t = 10$ days. After the reaxisymmetrization, the eddy diameter on the β plane was 314 km at $t = 27$ days. In general, the two features in the simulation were quite similar to the observations. Additionally, the numerical results indicated that the elliptical eddy rotated anticlockwise during the post-typhoon adjustment (more subfigures are omitted). The eddy moves northwestward in both the altimetry and simulated SSHA field owing to the β effect and nonlinear self-advection (Smith and O'Brien 1983).

Figure 2 illustrates the variation in the three-dimensional eddy structure, including the temporal evolution of temperature transitions along and across the track. Initially, the temperature anomaly (TA) of the COE

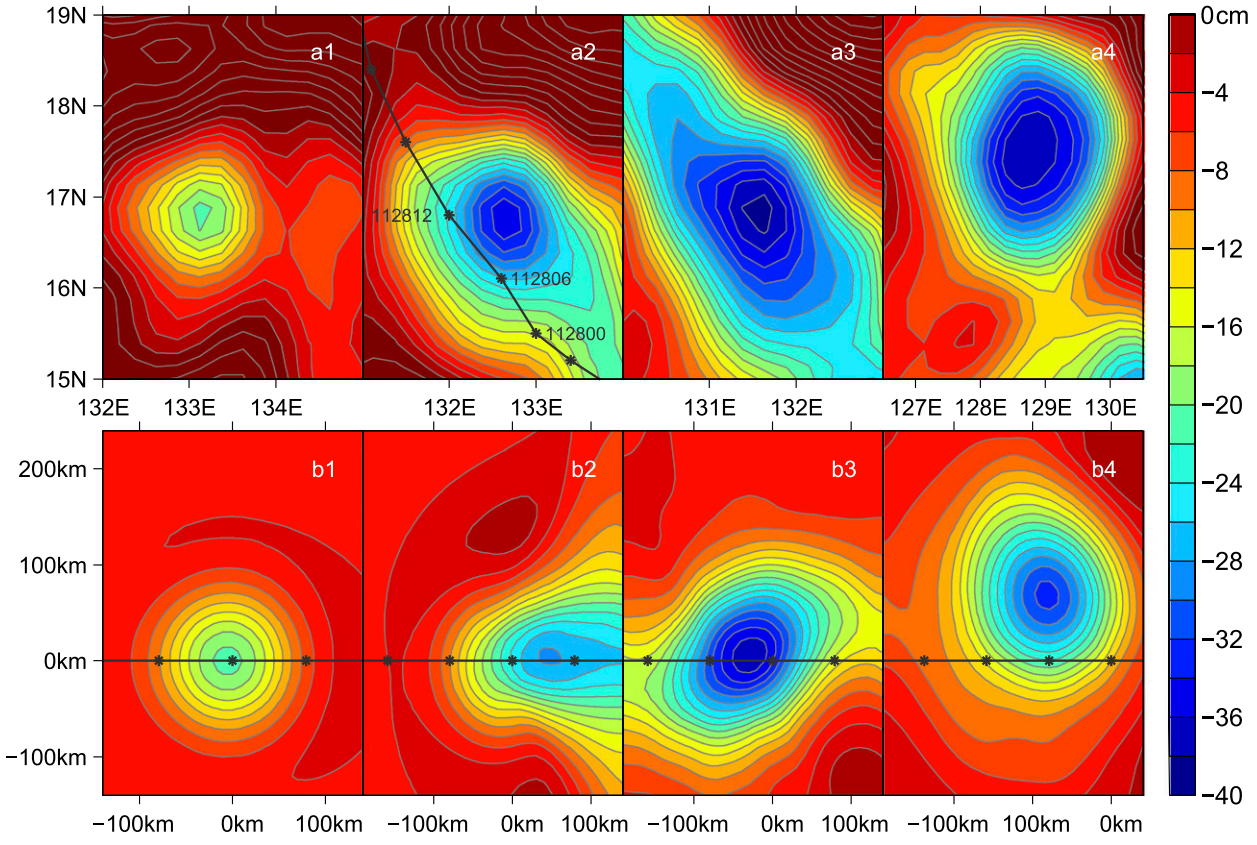

FIG. 1. SSHA features of the COE. (a),(b) SSHA distribution obtained from altimeter data and model output on the β plane, respectively. The four columns in (a) and (b) represent results at $t = -7$, 0, 10, and 30 days, respectively. Note that all of the data in (b) have had 6 cm subtracted. The real track of the typhoon is plotted in (a2), and the axis $y = 0$ in (b) is the track of the typhoon in the numerical model.

was axisymmetric with a maximum value of −1.0°C in the thermocline layer (Figs. 2a1, 2b1); 10 days after the typhoon passed, the maximum TA in the COE reached −2.8°C, approximately 3 times the initial value (−1.0°C). The thermocline temperature clearly demonstrated nonaxisymmetry because, despite a similar temperature reduction, the width across the track was smaller than that along the track (Figs. 2a2, 2b2, 2c1, 2c2). This implied the nonaxisymmetry of the isopycnal lifting and the elliptical deformation of the horizontal eddy shape. Note that the near-inertial wavelength is 434 km, according to the linear theory (Geisler 1970). The COE still had a −2.8°C temperature anomaly and was once again circular in shape 30 days after the typhoon passed (Figs. 2a3, 2b3, 2c1, 2c2).

The temperature variability at 100 m, both across and along the track, is illustrated in Fig. 2c. In the first couple of days, the isothermal lines shrank across the track but expanded along the track, which is an indirect indication of elliptical deformation. Then, the isothermal line expanded across the track and shrunk along the track after $t = 2$ days. The temporal evolution in Fig. 2c also demonstrated that the low temperature near the vortex center remained relatively unchanged for a long period of time after the typhoon caused the cooling of the thermocline layer to decline. The temperature response to the typhoon agreed with the behavior of the SSHA in Fig. 1. The reaxisymmetrization initially overshot the target at approximately 20 days and the COE reached a new balance at day 30 through a weak reverse adjustment (Fig. 2c), demonstrating the anticlockwise rotation of the elliptical eddy.

b. *Dynamic processes of the COE after a typhoon perturbation*

The eddy enhancement was likely due to the low-frequency component of typhoon-induced upwelling (Geisler 1970; Price 1983), which is different from the near-inertial pumping (Greatbatch 1984) and the influence of preexisting geostrophic vorticity (Jaimes and Shay 2009, 2015). This hypothesis was supported by the relationship between the eddy evolution and upwelling, shown in Fig. 3. The SSHA decreased shortly after the typhoon passed and then remained unchanged for some

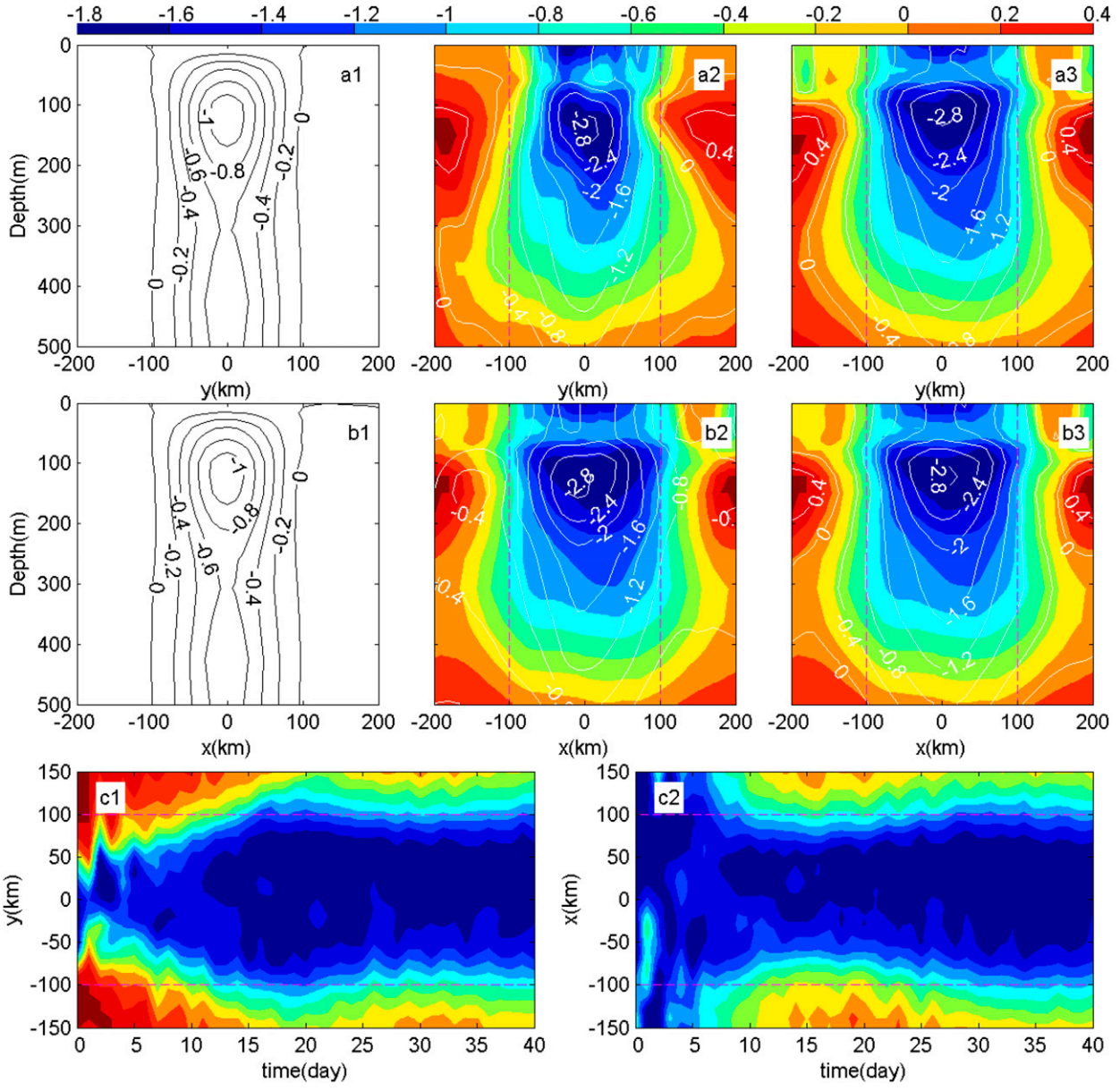

FIG. 2. The temperature distribution of the COE in the model output on the f plane. The contours denote the temperature anomalies (temperature fields subtracted from the climatological data) for (a) cross-track and (b) along-track sections. The color bars in (a) and (b) represent the temperature changes (temperature fields subtracted from the initial fields) induced by the typhoon for cross-track and along-track sections, respectively. The three columns in (a) and (b) represent the results at $t = -7$, 10, and 30 days, respectively. The temporal–spatial evolution of the temperature changes in (c1) cross-track and (c2) along-track directions at a depth of 100 m. The dash lines at $x = \pm 100$ km and $y = \pm 100$ km help to visualize the symmetry.

time. The SSHA variation due to the typhoon was also apparent in the time series of the simulated thermocline depths (Δh_{d20}, where h is the depth of isopycnal). Both the SSHA and Δh_{d20} suggest that the cyclonic eddy was indeed enhanced by the typhoon. We applied a Green function method, as described in Geisler (1970), with the wind stress profile to estimate the typhoon-induced upwelling. The most consistent period of low-frequency upwelling had a similar temporal evolution as the SSHA and the Δh_{d20}, suggesting that the low-frequency response enhanced the eddy (Fig. 3). The raised isopycnals that resulted from the theory were slightly stronger than the numerical model output because the theory neglects higher-mode response and mixed layer parameterization (Chang and Anthes 1978). It should be noted that the near-inertial internal wave did not propagate vertically

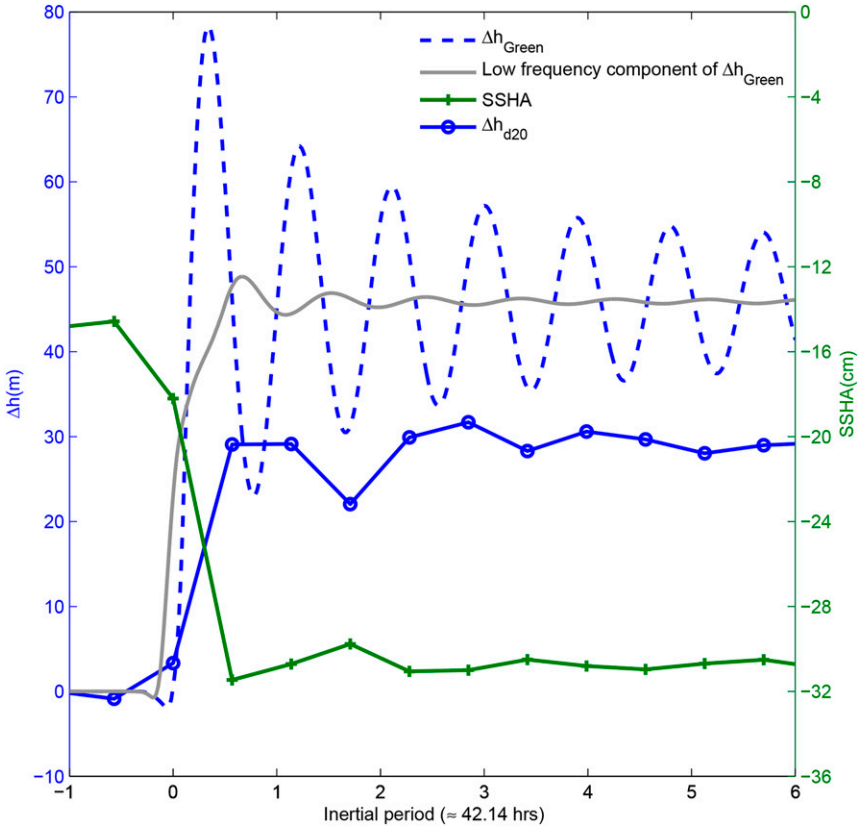

FIG. 3. The variation of the raised isopycnals and SSHA in the *f*-plane model output at the initial eddy center. The quantity Δh_{d20} is the raised 20°C isotherm as estimated from the model output. The value of Δh_{Green} was calculated with the Green function method in a two-layer linear model (Geisler 1970). The low-frequency component of Δh_{Green} was obtained by filtering the near-inertial internal waves. The Δ denotes the difference after and before the typhoon. Their initial values are calculated at a fixed time before the typhoon.

in a linear two-layer ocean and the near-inertial amplitude of Δh_{Green} decayed very slowly. In the real ocean, the amplitude would vanish after 7–8 inertial periods (Shay and Elsberry 1987; Jaimes and Shay 2010).

The deformation of the COE shape included two processes: from a circular to an elliptical shape and from an elliptical to a circular shape. The elliptical deformation of the initial circular eddy was related to the horizontal pattern of the low-frequency, typhoon-generated isopycnal lifting, which look like a ridge along the track (Geisler 1970). Along the track, the upwelling was consistently strong. Across the typhoon track, the upwelling was *e*-folding and decreased from the center of the COE with the length scale of the first baroclinic deformation radius. Thus, the horizontal pattern of upwelling across and along the track caused the circular eddy to become an elliptical one. The eddy diameter was enlarged along the track but decreased across the track. In other words, the major and minor axes of the ellipse were along and across the track, respectively. As a hyperbolic-type response, a fast-moving typhoon will diminish the strength of low-frequency response and reduce the ellipticity of COE (Geisler 1970). It is of note that the elliptical deformation of the COE is caused by vertical motion rather than the horizontal currents mentioned in Carton (2001).

Why does the elliptical eddy readjust to a circular shape after elliptical deformation? The process is similar to the axisymmetrization of the vertically tilted geostrophic vortex presented in Viera (1995). After the typhoon leaves, the flow surrounding the eddy forms a decaying turbulence system. The axisymmetric shape of an eddy can prevent potential enstrophy (i.e., PV variance) from cascading to dissipation scales and causing the death of vortices, while coherent vortices with local potential vorticity concentrations are long lived (McWilliams 1984). Thus, both the axisymmetrization and the vertical interaction, termed the vortex axis alignment, play an important role in the eddy evolution after the typhoon

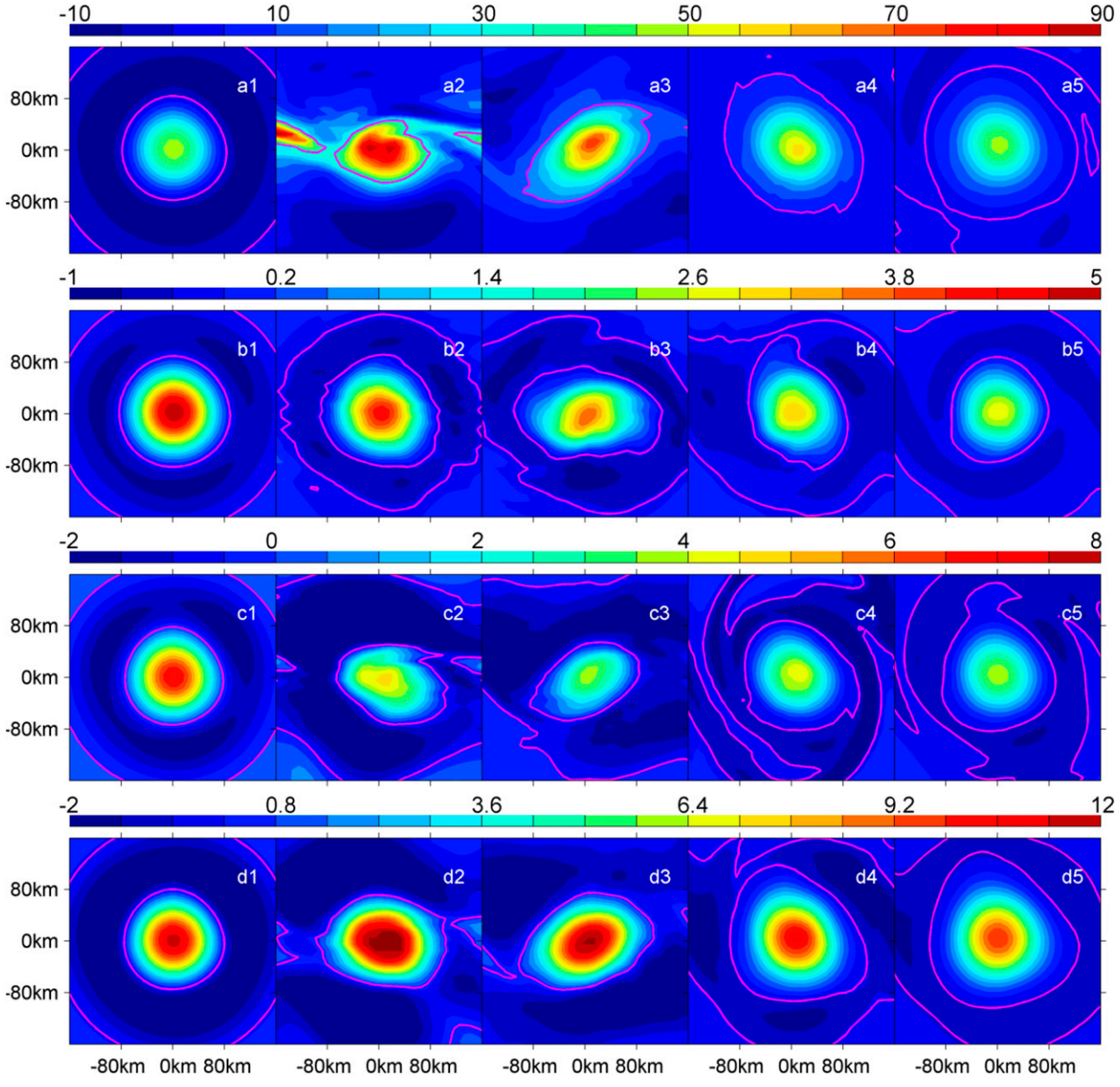

FIG. 4. (a),(b)The evolution of the PVA ($10^{-11}\,m^{-1}\,s^{-1}$) fields of two isopycnals $\sigma = 24$ and 26.7 represented in two planes: (c) the vertically integrated PVA ($10^{-8}\,s^{-1}$) and (d) the vertically integrated relative vorticity ($10^{-3}\,m\,s^{-1}$). The five columns illustrate the results at $t = -7$, 2, 10, 30, and 50 days, respectively. The pink line delineates the outermost closed contour of the PVA field. Note that the positive PVA field enclosed by the pink contour represents the core of the COE.

passes. Figure 4 shows the PVA fields on two isopycnals, $\sigma = 24$ and 26.7, diagnosed from the numerical output on the f plane, that were used to illustrate the eddy evolution in the thermocline layer and below thermocline layer (approximately 120 and 500 m). The typhoon injected a large amount of PV into the thermocline and concentrated more PV around the COE by input of relative vorticity (Fig. 4a2). Closed contours in the PVA field demonstrate the eddy distortion in the horizontal direction. The vortex in the thermocline rotated anticlockwise, spiraled into the original center, and became involved in some PV around the eddy. The PVA experienced a slight decay in the thermocline because the eddy entrains low PVA into the circle domain by stretching the water column and the corresponding PVA deficit feed to the surface layer. The area within the outermost closed contour increased until the eddy shape was once again a circle (Figs. 4a3,a4,a5). Additionally, the typhoon indirectly affected the eddy below the thermocline because there was no significant

deformation (Fig. 4b2). There was also a time lag between the rotation of the ellipse below the thermocline and the rotation within the thermocline itself (Fig. 4b3). Thus, there exists the pressure coupling between and below the thermocline, and the vortex shape below the thermocline readjusted to a circle to stop the potential enstrophy cascade. Because an elliptical vortex causes a potential enstrophy cascade into a smaller scale and dissipates its PV, the area within the outermost closed contour decreases (Fig. 4b5). In general, the evolution of the PVA demonstrated that the eddy grew in the thermocline and shrunk below the thermocline because of the typhoon, indicating that the typhoon affected the three-dimensional structure of the COE.

Vertical-integrated PVA and relative vorticity over the eddy depth is shown in Figs. 4c and 4d. Notably, the typhoon leads to the falloff of total PV in COE (Fig. 4c), while the typhoon injects relative vorticity into the COE to promote PV (Fig. 4d). The upwelling shown in Fig. 3 gives rise to the decay of total PV. The decrease of total PV indicates that the influence of upwelling is larger than that of relative vorticity for COE.

4. Conclusions

Both the SSHA and temperature field revealed that a typhoon can affect a COE by increasing its intensity and area and altering its 3D structure. The typhoon affected the COE by first causing an elliptical deformation and then an enhancement. The elliptic eddy gradually experienced reaxisymmetrization. The area of the COE within the thermocline increased, while the area below the thermocline decreased. These changes in the COE were due to the magnitude and horizontal pattern of upwelling and the dynamic processes of eddy adjustment.

This study demonstrates some new insights into the temporal and spatial evolution of a COE affected by external forces through some ideal experiments. The low-frequency response of the eddy to typhoon suggests that such a response may be important for local ocean dynamics. However, the other eddy type (anticyclonic), size, and strength were not accounted for this study. Further study is still need to explore the relationship between eddy structure and typhoon.

Acknowledgments. The study is supported by National Basic Research Program of China (2013CB430301 and 2013CB430303) and the Project GASI-IPOVAI-04, NSFC under Grants 41276023, 41376022, 41125019, and 41521005. We thank two anonymous reviewers for their help to improve the manuscript greatly.

REFERENCES

Benitez-Nelson, C. R., and Coauthors, 2007: Mesoscale eddies drive increased silica export in the subtropical Pacific Ocean. *Science*, **316**, 1017–1021, doi:10.1126/science.1136221.

Black, P. G., and G. J. Holland, 1995: The boundary layer of Tropical Cyclone Kerry (1979). *Mon. Wea. Rev.*, **123**, 2007–2028, doi:10.1175/1520-0493(1995)123<2007:TBLOTC>2.0.CO;2.

Bleck, R., 2002: An oceanic general circulation model framed in hybrid isopycnic-Cartesian coordinates. *Ocean Modell.*, **4**, 55–88, doi:10.1016/S1463-5003(01)00012-9.

Carton, X., 2001: Hydrodynamical modeling of oceanic vortices. *Surv. Geophys.*, **22**, 179–263, doi:10.1023/A:1013779219578.

Chang, S. W., and R. A. Anthes, 1978: Numerical simulations of the ocean's nonlinear, baroclinic response to translating hurricanes. *J. Phys. Oceanogr.*, **8**, 468–480, doi:10.1175/1520-0485(1978)008<0468:NSOTON>2.0.CO;2.

Chelton, D. B., M. G. Schlax, and R. M. Samelson, 2011: Global observations of nonlinear mesoscale eddies. *Prog. Oceanogr.*, **91**, 167–216, doi:10.1016/j.pocean.2011.01.002.

Geisler, J. E., 1970: Linear theory of the response of a two layer ocean to a moving hurricane. *Geophys. Astrophys. Fluid Dyn.*, **1**, 249–272, doi:10.1080/03091927009365774.

Greatbatch, R. J., 1984: On the response of the ocean to a moving storm: Parameters and scales. *J. Phys. Oceanogr.*, **14**, 59–78, doi:10.1175/1520-0485(1984)014<0059:OTROTO>2.0.CO;2.

Jaimes, B., and L. K. Shay, 2009: Mixed layer cooling in mesoscale oceanic eddies during Hurricanes Katrina and Rita. *Mon. Wea. Rev.*, **137**, 4188–4207, doi:10.1175/2009MWR2849.1.

——, and ——, 2010: Near-inertial wave wake of Hurricanes Katrina and Rita over mesoscale oceanic eddies. *J. Phys. Oceanogr.*, **40**, 1320–1337, doi:10.1175/2010JPO4309.1.

——, and ——, 2015: Enhanced wind-driven downwelling flow in warm oceanic eddy features during the intensification of Tropical Cyclone Isaac (2012): Observations and theory. *J. Phys. Oceanogr.*, **45**, 1667–1689, doi:10.1175/JPO-D-14-0176.1.

——, ——, and G. R. Halliwell, 2011: The response of quasigeostrophic oceanic vortices to tropical cyclone forcing. *J. Phys. Oceanogr.*, **41**, 1965–1985, doi:10.1175/JPO-D-11-06.1.

Legal, C., P. Klein, A.-M. Treguier, and J. Paillet, 2007: Diagnosis of the vertical motions in a mesoscale stirring region. *J. Phys. Oceanogr.*, **37**, 1413–1424, doi:10.1175/JPO3053.1.

McWilliams, J. C., 1984: The emergence of isolated coherent vortices in turbulent flow. *J. Fluid Mech.*, **146**, 21–43, doi:10.1017/S0022112084001750.

Price, J. F., 1983: Internal wave wake of a moving storm. Part I: Scales, energy budget and observations. *J. Phys. Oceanogr.*, **13**, 949–965, doi:10.1175/1520-0485(1983)013<0949:IWWOAM>2.0.CO;2.

Schade, L. R., and K. A. Emanuel, 1999: The ocean's effect on the intensity of tropical cyclones: Results from a simple coupled atmosphere–ocean model. *J. Atmos. Sci.*, **56**, 642–651, doi:10.1175/1520-0469(1999)056<0642:TOSEOT>2.0.CO;2.

Shang, X., H. Zhu, G. Chen, C. Xu, and Q. Yang, 2015: Research on cold core eddy change and phytoplankton bloom induced by typhoons: Case studies in the South China Sea. *Adv. Meteor.*, **2015**, 340432, doi:10.1155/2015/340432.

Shay, L. K., and R. L. Elsberry, 1987: Near-inertial ocean current response to Hurricane Frederic. *J. Phys. Oceanogr.*, **17**, 1249–1269, doi:10.1175/1520-0485(1987)017<1249:NIOCRT>2.0.CO;2.

Smith, D. C., and J. O'Brien, 1983: The interaction of a two-layer isolated mesoscale eddy with bottom topography. *J. Phys. Oceanogr.*, **13**, 1681–1697, doi:10.1175/1520-0485(1983)013<1681:TIOATL>2.0.CO;2.

Sun, L., Y. Yang, T. Xian, Z. Lu, and Y. Fu, 2010: Strong enhancement of chlorophyll a concentration by a weak typhoon. *Mar. Ecol. Prog. Ser.*, **404**, 39–50, doi:10.3354/meps08477.

——, ——, ——, Y. Wang, and Y.-F. Fu, 2012: Ocean responses to Typhoon Namtheun explored with Argo floats and multiplatform satellites. *Atmos.–Ocean*, **50**, 15–26, doi:10.1080/07055900.2012.742420.

——, Y.-X. Li, Y.-J. Yang, Q. Wu, X.-T. Chen, Q.-Y. Li, Y.-B. Li, and T. Xian, 2014: Effects of super typhoons on cyclonic ocean eddies in the western North Pacific: A satellite data-based evaluation between 2000 and 2008. *J. Geophys. Res. Oceans*, **119**, 5585–5598, doi:10.1002/2013JC009575.

Viera, F., 1995: On the alignment and axisymmetrization of a vertically tilted geostrophic vortex. *J. Fluid Mech.*, **289**, 29–50, doi:10.1017/S0022112095001224.

Walker, N. D., R. R. Leben, and S. Balasubramanian, 2005: Hurricane-forced upwelling and chlorophyll a enhancement within cold-core cyclones in the Gulf of Mexico. *Geophys. Res. Lett.*, **32**, L18610, doi:10.1029/2005GL022388.

——, ——, C. T. Pilley, M. Shannon, D. C. Herndon, I.-F. Pun, I.-I. Lin, and C. L. Gentemann, 2014: Slow translation speed causes rapid collapse of northeast Pacific Hurricane Kenneth over cold core eddy. *Geophys. Res. Lett.*, **41**, 7595–7601, doi:10.1002/2014GL061584.

Zhang, Z., Y. Zhang, W. Wang, and R. X. Huang, 2013: Universal structure of mesoscale eddies in the ocean. *Geophys. Res. Lett.*, **40**, 3677–3681, doi:10.1002/grl.50736.

Zheng, Z.-W., C.-R. Ho, and N.-J. Kuo, 2008: Importance of pre-existing oceanic conditions to upper ocean response induced by Super Typhoon Hai-Tang. *Geophys. Res. Lett.*, **35**, L20603, doi:10.1029/2008GL035524.

——, ——, Q. Zheng, Y.-T. Lo, N.-J. Kuo, and G. Gopalakrishnan, 2010: Effects of preexisting cyclonic eddies on upper ocean responses to Category 5 typhoons in the western North Pacific. *J. Geophys. Res.*, **115**, C09013, doi:10.1029/2009JC005562.